Carbon nanotube population analysis from Raman and photoluminescence intensities

A. Jorio, C. Fantini, and M. A. Pimenta
Departamento de Física, Universidade Federal de Minas Gerais, Belo Horizonte, Minas Gerais, 30123-970 Brazil

D. A. Heller and M. S. Strano
Department of Chemistry, Department of Chemical and Biomolecular Engineering, University of Illinois at Urbana/Champaign, 118 Roger Adams Laboratory, Box C-3 600 South Mathews Avenue, Urbana, Illinois 61801-3602

M. S. Dresselhaus
Department of Physics and Department of Electrical Engineering and Computer Science, Massachusetts Institute of Technology, Cambridge, Massachusetts 02139-4307

Y. Oyama, J. Jiang, and R. Saito
Department of Physics, Tohoku University and CREST JST, Aoba Sendai 980-8578, Japan

(Received 25 July 2005; accepted 11 November 2005; published online 11 January 2006)

In the absence of standard single-wall carbon nanotube samples with a well-known (n,m) population, we provide both a photoluminescence excitation (PLE) and resonance Raman scattering (RRS) analysis that together can be used to check the calculations for PLE and RRS intensities for carbon nanotubes. We compare our results with available models and show that they describe well the chirality dependence of the intensity ratio, confirming the differences between type 1 and type 2 semiconducting tubes $[(2n+m) \bmod 3]=1$ and 2, respectively, and the existence of a node in the radial breathing mode intensity for type 2 carbon nanotubes with chiral angles between 20° and 25°. © *2006 American Institute of Physics*. [DOI: 10.1063/1.2162688]

Large efforts are now being directed to developing synthesis or manipulation processes able to generate single-wall carbon nanotubes (SWNTs) with well-defined geometric structure, i.e., diameter (d_t) and chiral angle (θ), or equivalently their (n,m) indices.[1–3] Photoluminescence excitation[2,4] (PLE) and resonance Raman spectroscopy[5–7] (RRS) are two techniques able to nondestructively probe isolated tubes and large ensembles, characterizing the result of a given synthesis or separation process, giving the (n,m) values of the samples using optical techniques. Since the RRS and PLE intensities depend on the number of scatterers in the sample, intensity analysis provides the population of specific (n,m) SWNTs in the sample.[8–10] However, since the efficiency for the RRS and PLE processes should also depend on (n,m), the population information cannot be extracted directly from the measured intensities, but should firstly be corrected to account for the (n,m) dependence of the RRS and PLE efficiencies.[9,10]

To make such corrections for the (n,m) dependence of the RRS and PLE intensities, different calculations have been performed.[11–15] However, due to the lack of a sample with a well-known (n,m) population, there is no experimental evaluation of the accuracy of the proposed models. In this paper we provide experimental results that can be used to evaluate the RRS and PLE intensity calculations. We measure both RRS and PLE on a SWNT sample and we propose that the experimental intensity ratio $I_{\mathrm{Exp}}^{\mathrm{PLE}}/I_{\mathrm{Exp}}^{\mathrm{RRS}}$ should be independent of the (n,m) population. This ratio can, therefore, be used to test the validity and accuracy of the calculated intensity ratio $I_{\mathrm{Calc}}^{\mathrm{PLE}}/I_{\mathrm{Calc}}^{\mathrm{RRS}}$.

The RRS and PLE experiments were performed at room temperature on HiPco SWNTs in SDS suspended aqueous solution, prepared as described in Ref. 16. For the RRS experiments, a Dilor *XY* triple monochromator equipped with a N_2-cooled charge-coupled device (CCD) was used and excited by ArKr, Ti:Sapphire and dye lasers in the range 1.6 to 2.7 eV. The reported data for RRS intensities $(I_{\mathrm{Exp}}^{\mathrm{RRS}})$ are related to resonances with the E_{22}^S nanotube levels.[6] For PLE experiments, we used a home-built *n*-IR fluorescence spectrometer, coupled to a nitrogen-cooled germanium detector (Edinburgh Instruments). The excitation ranged between 1.55 to 3.10 eV, and nanotube emission was measured between 0.89 to 1.38 eV. The reported data for PLE intensities $(I_{\mathrm{Exp}}^{\mathrm{PLE}})$ are related to absorption at E_{22}^S and emission at E_{11}^S levels.[4] The spectral intensities [$I_{\mathrm{Exp}}^{\mathrm{RRS}}$ for RRS and $I_{\mathrm{Exp}}^{\mathrm{PLE}}$ for PLE (see Table I)] were evaluated from the radial breathing mode (RBM) RRS profile[6] and from the PLE resonance profile[4,8] for each (n,m) tube. The RRS intensities are calibrated by measuring the signal of nonresonant CCl_4 under the same conditions. The PLE intensities are calibrated by dividing the nanotube signal over the relative lamp power at all excitation wavelengths and by considering the blackbody spectrum.

A given PLE or RRS experimental intensity accuracy is basically related to the strength of the signal and the number of different excitation laser lines close enough in energy so that the resonance profile can be well evaluated. This profile can change from tube to tube and, in our case, the accuracy is better than 20%. When comparing the (n,m) dependence for the $I_{\mathrm{Exp}}^{\mathrm{PLE}}$ data obtained in this paper with published data for HiPco SWNTs (e.g., by Bachilo *et al.*[8]), the overall (n,m) dependence is similar. Some intensity differences go up to 30% of the values and these differences can be related to

TABLE I. Normalized spectral intensities (I_{Exp}^{RRS} for RRS and I_{Exp}^{PLE} for PLE) obtained experimentally for 22 HiPco SWNTs in SDS suspended aqueous solution [see Refs. 6, 9, and 10 for excitation laser energy and radial breathing mode frequency of each (n,m) SWNT]. The (n,m) dependent RRS (I_{Calc}^{RRS}) and PLE (I_{Calc}^{PLE}) normalized theoretical intensities (see text) are also given.

(n,m)	I_{Exp}^{RRS}	I_{Exp}^{PLE}	I_{Calc}^{RRS}	I_{Calc}^{PLE}	(n,m)	I_{Exp}^{RRS}	I_{Exp}^{PLE}	I_{Calc}^{RRS}	I_{Calc}^{PLE}
(6,4)	0.13	0.00	0.51	1.00	(9,4)	0.54	0.70	0.47	0.30
(6,5)	0.16	0.29	0.08	0.75	(9,7)	0.03	0.76	0.12	0.18
(7,5)	0.90	0.60	0.31	0.58	(10,2)	0.64	0.44	0.73	0.26
(7,6)	0.16	0.73	0.04	0.42	(10,3)	0.26	0.60	0.12	0.09
(8,3)	1.00	0.18	0.71	0.54	(10,5)	0.08	0.86	0.31	0.24
(8,4)	0.01	0.53	0.01	0.28	(11,1)	0.56	0.51	0.27	0.02
(8,6)	0.18	1.00	0.19	0.25	(11,3)	0.11	0.72	0.54	0.21
(8,7)	0.04	0.95	0.03	0.24	(11,4)	0.02	0.47	0.08	0.08
(9,1)	0.08	0.00	1.00	0.42	(12,1)	0.13	0.46	0.68	0.15
(9,2)	0.08	0.23	0.18	0.13	(13,3)	0.02	0.33	0.15	0.03
(9,5)	0.01	0.80	0.01	0.17	(14,1)	0.03	0	0.23	0.01

differences in sample population due to different sample preparation procedures.

The experimental results will be here compared to theoretical calculations. The PLE theoretical intensities [I_{Calc}^{PLE} (see Table I)] are calculated by the product of the E_{22}^S induced absorption probability, the electron relaxation rate from E_{22}^S state to any other state satisfying energy-momentum conservation by emitting or absorbing one phonon at 300 K, and the E_{11} spontaneous emission probability, as described in Ref. 14. Reich *et al.*[15] used a different model to calculate PL intensities, but the general (n,m) dependence is similar to what is shown here and does not change the conclusions, as discussed later. The RRS theoretical intensities [I_{Calc}^{RRS} (see Table I)] were calculated using the procedure discussed in Refs. 11 and 12, making use of the symmetry-adapted nonorthogonal tight-binding model and considering resonance with E_{22}^S levels. The results used here are in good agreement with *ab initio* calculations for the electron-phonon coupling.[13]

The analysis we propose is now discussed. Figures 1 and 2 show the intensity ratios between the corresponding PLE and RRS data for type 1 and type 2 semiconducting SWNTs, respectively. While both the RRS and PLE intensities depend on the number of each specific (n,m) SWNT in the sample, the ratio should be population independent and can be compared to the intensity ratio calculation. The upper panels show $I_{Calc}^{PLE}/I_{Calc}^{RRS}$, and the lower panels show $I_{Exp}^{PLE}/I_{Exp}^{RRS}$. For type 1 SWNTs, Fig. 1 shows that the predicted chirality dependence for the intensity ratio $I_{Calc}^{PLE}/I_{Calc}^{RRS}$ is indeed seen in the experimental ratio $I_{Exp}^{PLE}/I_{Exp}^{RRS}$, i.e., the ratio increases with increasing chiral angle. The diameter dependence, however, seems not to be well described by the theory. While a strong increase in $I_{Exp}^{PLE}/I_{Exp}^{RRS}$ is observed for increasing diameter, a basically d_t independent $I_{Calc}^{PLE}/I_{Calc}^{RRS}$ is predicted, since the I_{Calc}^{PLE} and I_{Calc}^{RRS} exhibit similar diameter dependencies that approximately cancel each other in taking the ratio. This experimental result indicates that the d_t dependencies of either I_{Calc}^{PLE} or I_{Calc}^{RRS} (or maybe both) are not correctly described by theory.

For type 2 SWNTs, Fig. 2 shows a similar problem in describing the diameter dependence of the intensity ratios. Regarding the chirality dependence, Fig. 2 shows a remarkable result, which is the very large intensity ratios observed for the same two SWNTs—the (8,4) and the (9,5)—in both the calculated and experimental plots. From theory, these large $I_{Calc}^{PLE}/I_{Calc}^{RRS}$ values come from the very small values of I_{Calc}^{RRS} for these two SWNTs, due to a predicted node in the electron-phonon coupling for type 2 SWNTs with chiral angle between 20° and 25° (depending on E_{ii}).[12] The experimental ratio, therefore, confirms the theoretical prediction of this node.

In conclusion, in the absence of standard single-wall carbon nanotubes samples with a well-known (n,m) population, we provide a PLE *and* RRS analysis that can be used to check the calculation for the PLE and RRS intensity. From our analysis, we conclude that the theoretical calculations

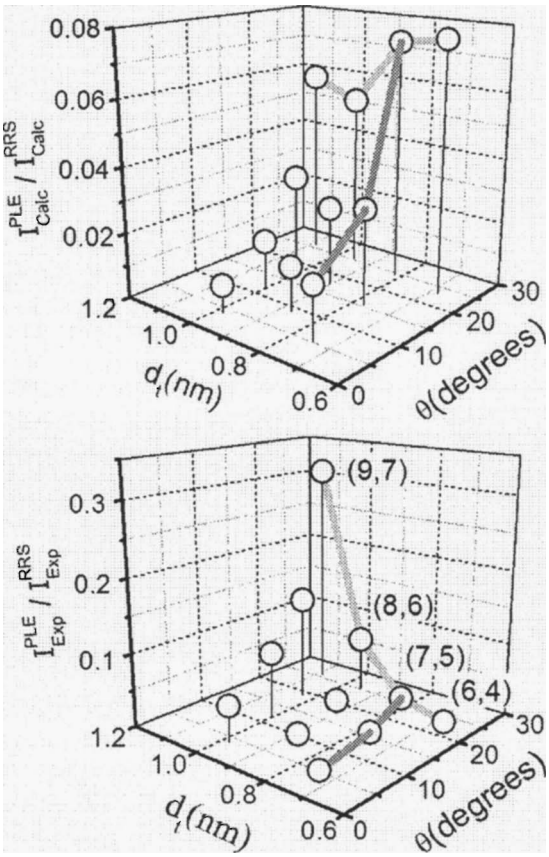

FIG. 1. Upper panel, calculated $I_{Calc}^{PLE}/I_{Calc}^{RRS}$ intensity ratio; lower panel, experimental $I_{Exp}^{PLE}/I_{Exp}^{RRS}$ intensity ratio, both for SWNTs with $(2n+m)\bmod 3$ equals 1 (type 1), as a function of diameter and chiral angle. The broad dark gray lines connect SWNTs with the same $(2n+m)$ (similar d_t) and the broad light gray lines connect SWNTs with the same $(n-m)$ (similar θ). For each $(2n+m)$=constant family (similar d_t), one (n,m) SWNT is assigned.

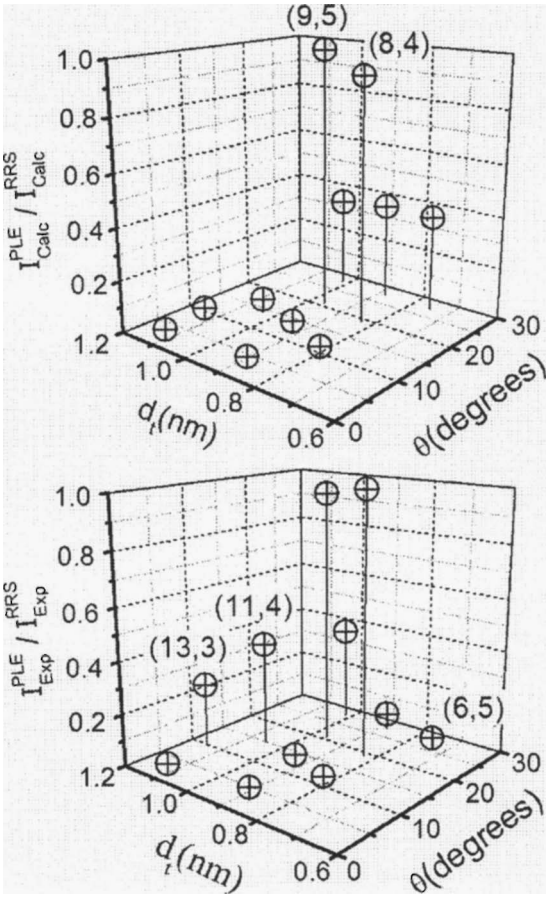

FIG. 2. Upper panel, calculated $I^{PLE}_{Calc}/I^{RRS}_{Calc}$ intensity ratio; lower panel, experimental $I^{PLE}_{Exp}/I^{RRS}_{Exp}$ intensity ratio, both for SWNTs with $(2n+m)\mathrm{mod}\,3$ equals 2 (type 2), as a function of diameter and chiral angle. For each $(2n+m)$=constant family (similar d_t), one (n,m) SWNT is assigned.

discussed here describe the chirality dependence of the PLE and RRS intensities very well, including the type 1 versus type 2 difference and the presence of a node in the RBM RRS for type 2 SWNTs with chiral angles between 20° and 25°. These results are important to validate recent population characterization on HiPco (Ref. 10) and CoMoCAT (Ref. 9) SWNTs. In both samples, a preferential production of large chiral angle tubes was observed for low diameter tubes ($d_t < 0.9$ nm).[9,10] In a CoMoCAT sample, the identification by RRS of the (6,5) SWNT as the most abundant tube in the sample depends strongly on the theoretical correction, since this is a type 2 tube with a chiral angle $\theta=27°$, close to the predicted RBM RRS intensity node.[9]

The diameter dependence of the PLE and RRS intensities, however, is underestimated by the models. This result suggests the need of including exciton formation in the intensity calculation formalism, since excitonic effects are known to depend strongly on diameter but weakly on chirality.[17,18] An exciton-based model has been proposed in the literature to describe the photoluminescence intensity in SWNTs,[15] but the general prediction from this model is similar to the result analyzed here.[14] The analysis performed here cannot be used to support one PL model rather than the other model, but our analysis may suggest that the underestimated diameter dependence of the PLE/RRS intensity ratio is related to an excitonic effect not included in the RRS calculations.

A.J. acknowledges J.P.V. Macena for helpful work. Authors A.J., C.F., and M.A.P. acknowledge financial support by PRPq-UFMG, FAPEMIG, and CNPq. M.S.S. acknowledges funding from the U.S. National Science Foundation Grant No. NIRT ECS 04-03489 and a CAREER award CTS-0449147. R.S. acknowledges a Grant-in-Aid (No. 16076201) from the Ministry of Education Science, Sports, and Culture Japan. M.S.D. acknowledges support under NSF Grant No. DMR 04-05538.

[1] M. J. Bronikowsky, P. A. Willis, D. T. Colbert, K. A. Smith, and R. E. Smalley, J. Vac. Sci. Technol. A **19**, 1800 (2001).
[2] S. Maruyama, Y. Mihauchi, Y. Murakami, and S. Chiashi, New J. Phys. **5**, 149 (2003).
[3] B. Kitiyanan, W. E. Alvarez, J. H. Harwell, and D. E. Resasco, Chem. Phys. Lett. **317**, 497 (2000).
[4] S. M. Bachilo, M. S. Strano, C. Kittrell, R. H. Hauge, R. E. Smalley, and R. B. Weisman, Science **298**, 2361 (2002).
[5] A. Jorio, R. Saito, J. H. Hafner, C. M. Lieber, M. Hunter, T. McClure, G. Dresselhaus, and M. S. Dresselhaus, Phys. Rev. Lett. **86**, 1118 (2001).
[6] C. Fantini, A. Jorio, M. Souza, M. S. Strano, M. S. Dresselhaus, and M. A. Pimenta, Phys. Rev. Lett. **93**, 147406 (2004).
[7] S. K. Doorn, D. A. Heller, P. W. Barone, M. L. Usrey, and M. S. Strano, Appl. Phys. A: Mater. Sci. Process. **78**, 1147 (2004).
[8] S. M. Bachilo, L. Balzano, J. E. Herrera, F. Pompeo, D. E. Resasco, and R. B. Weisman, J. Am. Chem. Soc. **125**, 11186 (2003).
[9] A. Jorio, A. P. Santos, H. B. Ribeiro, C. Fantini, M. Souza, J. P. M. Vieira, C. A. Furtado, J. Jiang, R. Saito, L. Balzano, D. E. Resasco, and M. A. Pimenta, Phys. Rev. B **72**, 075207 (2005).
[10] A. Jorio, C. Fantini, M. A. Pimenta, R. B. Capaz, Ge. G. Samsonidze, G. Dresselhaus, M. S. Dresselhaus, J. Jiang, N. Kobayashi, A. Grüneis, and R. Saito, Phys. Rev. B **71**, 075401 (2005).
[11] V. N. Popov, L. Henrard, and P. Lambin, Nano Lett. **4**, 1795 (2004).
[12] J. Jiang, R. Saito, A. Grüneis, S. G. Chou, Ge. G. Samsonidze, A. Jorio, G. Dresselhaus, and M. S. Dresselhaus, Phys. Rev. B **71**, 205420 (2005).
[13] M. Machón, S. Reich, H. Telg, J. Maultzsch, P. Ordejón, and C. Thomsen, Phys. Rev. B **71**, 035416 (2005).
[14] Y. Oyama, R. Saito, K. Sato, J. Jiang, Ge. G. Samsonizde, A. Grüneis, Y. Miyauchi, S. Maruyama, A. Jorio, G. Dresselhaus, and M. S. Dresselhaus, Carbon (to be published).
[15] S. Reich, C. Thomsen, and J. Robertson, Phys. Rev. Lett. **95**, 077402 (2005).
[16] M. J. O'Connell, S. M. Bachilo, X. B. Huffman, V. C. Moore, M. S. Strano, E. H. Haroz, K. L. Rialon, P. J. Boul, W. H. Noon, C. Kittrell, J. Ma, R. H. Hauge, R. B. Weisman, and R. E. Smalley, Science **297**, 593 (2002).
[17] H. Zhao and S. Mazumdar, Phys. Rev. Lett. **93**, 157402 (2004).
[18] C. L. Kane and E. J. Mele, Phys. Rev. Lett. **93**, 197402 (2004).